Talanta 94 (2012) 295–300

Contents lists available at SciVerse ScienceDirect

Talanta

journal homepage: www.elsevier.com/locate/talanta

Rhodamine 6G conjugated-quantum dots used for highly sensitive and selective ratiometric fluorescence sensor of glutathione

Rijun Gui[a], Xueqin An[a,*], Hongjuan Su[a], Weiguo Shen[a], Linyong Zhu[b], Xingyuan Ma[c], Zhiyun Chen[a], Xiaoyong Wang[a]

[a] Department of Physical Chemistry, College of Chemistry and Molecular Engineering, East China University of Science and Technology, Shanghai 200237, PR China
[b] Key Laboratory for Advanced Materials, Institute of Fine Chemicals, East China University of Science and Technology, Shanghai 200237, PR China
[c] State Key Laboratory of Bioreactor Engineering, New World Institute of Biotechnology, East China University of Science and Technology, Shanghai 200237, PR China

ARTICLE INFO

Article history:
Received 14 January 2012
Received in revised form 12 March 2012
Accepted 22 March 2012
Available online 29 March 2012

Keywords:
Quantum dots
Fluorescence
Glutathione
Ratiometric sensor

ABSTRACT

Rhodamine 6G (R6G) and 3-mercaptopropionic acid (MPA) capped-CdTe quantum dots (QDs) were conjugated by electrostatic interactions in aqueous solution. The R6G-QDs conjugate was utilized as a photoluminescence (PL) ratiometric sensor for the detection of glutathione (GSH). In this method, intentional introduction of GSH destroyed the conjugation of R6G and QDs, and induced regular PL change of R6G-QDs conjugates due to the competitive chelation between GSH and MPA ligand on the surface of QDs. The ratio of PL intensity of R6G (I_{R6G}) to that of QDs (I_{QDs}) in this conjugate was near linear toward the concentration of GSH in the range from 0.05 to 80 μM, and corresponding regression equation showed a good linear coefficient of 0.9954. The limit of detection of 15 nM in this proposed method was about 40-fold lower than that of other QDs-based PL sensors. Interferential experiments testified that R6G-QDs conjugates-based ratiometric PL sensor of GSH showed high selectivity over other related thiols and amino acids. Real sample assays further verified perfect analysis performance of the PL sensor of GSH. In comparison with conventional analytical techniques for the measurement of GSH, this ratiometric PL sensor was facile, economic, highly sensitive and selective.

© 2012 Elsevier B.V. All rights reserved.

1. Introduction

Tripeptide reduced glutathione (GSH), as biothiols or low-molecular-mass thiols, abundantly presents in cells of many different organisms and plays a pivotal role in maintaining reducing environment of cells [1,2]. Hence, the detection of GSH becomes significant for evaluating cellular functions. Conventional analytical techniques, such as spectrophotometry, electrochemistry, capillary electrophoresis, gas chromatography and high performance liquid chromatography (HPLC), have been exploited to determine GSH in biological samples, but these technologies are specific, expensive and time-consuming, in company with relatively complex processes in practical applications [3–8].

During the past decade, spectrofluorimetric methods were of great interest due to their sensitivity, simplicity and low cost [9–26]. Therein, organic dyes were usually used as a PL probe in detection systems of GSH. Nevertheless, among these probes, chemical reactions between organic dyes and the —SH of thiols partly weakened the selectivity of this determination. In addition, organic dyes were vulnerable to photobleaching, which made specific detection of GSH more difficult. By contrast, high-quality photoluminescence (PL) quantum dots (QDs) probably conquer this limitation. Unique properties of QDs, such as the broad excitation and size-tunable PL spectra, relatively high quantum yield and photochemical stability, allow QDs-based PL sensors to generate a distinct target signal for the qualitative or quantificational analysis of various substances [9–15].

To date, to the best of our knowledge, only two reports have referred to QDs-based sensors for quantificational detection of GSH. Wang et al. designed a graphene oxide amplified electrogenerated chemiluminescence of QDs platform for selective sensing of GSH in the range from 24 to 214 μM with a limit of detection (LOD) of 8.3 μM [27]. Liu et al. utilized CdSe-ZnS QDs-based OFF-ON fluorescence probes to selectively detect GSH (5–250 μM, LOD = 0.6 μM) [28]. In previous reports, basic principles of QDs-based sensors were attributed to the quenching or enhancement of PL signal. However, it is rather difficult to acquire exact PL intensity in real samples because of PL fluctuations in reagent concentration and intrinsic background PL. To overcome this defect, ratiometric sensors were developed by introducing a second chromophore, so that the ratiometric PL signal is independent of sensors' concentration.

Although QDs-based ratiometric PL sensors have been developed to sensitively detect pH and metal ions (such as Cu^{2+}) in recent years, this typical sensor-based detection of GSH is still

* Corresponding author. Tel.: +86 21 6425 0804; fax: +86 21 6425 2012.
E-mail addresses: anxueqin@ecust.edu.cn, jacky_0538@163.com (X. An).

0039-9140/$ – see front matter © 2012 Elsevier B.V. All rights reserved.
http://dx.doi.org/10.1016/j.talanta.2012.03.043

rarely reported [29–31]. Most recently, Kim and co-workers prepared a coumarin derivative with a hydrogen bond for the detection of GSH, based on a rapid and ratiometric fluorescence imaging [32]. However, this method could be applied as a qualitative, but not a quantificational sensing of GSH.

Herein, we attempted to achieve a novel PL sensor for quantificational detection of GSH, based on conjugates of rhodamine 6G (R6G) and 3-mercaptopropionic acid (MPA) capped-CdTe QDs (R6G-QDs), formed by electrostatic interactions in aqueous solution. In following experiments, a linear relationship between the ratio of PL intensity (I_{R6G}/I_{QDs}) and the concentration of GSH (C_{GSH}) would be achieved. According to this relationship, a novel method for the determination of GSH could be put forward. Compared with previous GSH assay protocols, this proposed method was facile, rapid, low-cost, highly sensitive and selective. It would be developed to determine the C_{GSH} in biological samples or relatively complicated systems.

2. Experimental

2.1. Materials

$CdCl_2{\cdot}2.5H_2O$ (99%) and $NaBH_4$ (99%) were obtained from Shanghai Reagent Company of China. Tellurium power (99.999%, ~200 mesh), Bovine serum albumin (BSA, ~66.43 KDa), MPA and R6G were purchased from Aldrich. Aqueous liposome solutions (~100 nM in diameter) were prepared utilizing the method of Ref. [33]. Other chemicals were of analytical grade and all chemicals were used directly as received without any purification. Ultrapure water with a resistivity of 18.2 ΩM cm^{-1} (Millipore Simplicity, USA) was used in all experiments. 10 mM of phosphate buffer solution (PBS, pH 7.0), consisting of 6.1 mM of Na_2HPO_4 and 3.9 mM of KH_2PO_4, was prepared firstly. Accordingly, a series of 10 mM of PBS with the pH from 5.0 to 9.0 were obtained by adjusting the concentration ratio of Na_2HPO_4 and KH_2PO_4.

2.2. Apparatus

UV–vis spectra were recorded with a Shimadzu UV-2450 UV–vis spectrophotometer. Fluorescence spectra measurement was performed with a FLSP 920 fluorescence spectrophotometer (Edinburgh Instruments) with a Xe lamp used for excitation at room temperature. Fluorescence lifetime study was performed using an Edinburgh FL nF900 mode single-photon counting system equipped with a H_2 lamp as the excitation resource. A 1 cm path length quartz cuvette was utilized in all measurements. Fourier transform infrared (FTIR) measurements on powdered samples were made using a Nicolet 6700 FTIR spectrometer in transmission mode with a KBr window. The HPLC spectroscopy meter (Agilent 1100) was utilized to detect the concentration of GSH. Dynamic light scattering (DLS) analysis was conducted with Zeta Sizer nano series laser light scattering system (Malvern Instrument Corporation).

2.3. Preparation of MPA-capped CdTe QDs

Firstly, NaHTe precursor was synthesized by the redox reaction of tellurium power and $NaBH_4$ according to the procedure reported in Ref. [34]. Then, CdTe QDs were prepared with a modified method of the Ref. [35]. Briefly, 50 mL aqueous solution, containing 0.25 mmol of Cd^{2+} and 0.43 mmol of MPA, was placed in a three-necked flash, adjusting the pH of this mixture to 12 via drop by drop adding 1.0 M of NaOH. Under the protection of N_2, freshly prepared 0.025 mmol of NaHTe solution was injected swiftly with a syringe into this mixture at room temperature. The mixture was heated to reflux with a condenser attached at 100 °C. Aliquots of the production were taken out at different time intervals to record temporal evolution of UV–vis and fluorescence spectrum. When the expected fluorescence wavelength was observed, following work was to remove the heating source and cool this mixture to room temperature. Afterward, prepared CdTe QDs was concentrated by circumrotate evaporation, precipitated with 2-propanol and collected by centrifugation. The colloidal precipitate was dried in vacuum at 60 °C and grinded to acquire CdTe QDs dry powder for solid analysis, or dispersed in aqueous solution for applications in subsequent experiments.

2.4. Fabrication and PL characterization of R6G-QDs conjugates

Aliquots of prepared MPA capped-CdTe QDs were dispersed in 10 mM PBS (pH 7.4). The concentration of QDs was adjusted to 5, 10, 15, 20, 25, 35 and 50 nM, respectively, calculated by empirical mathematical functions in Ref. [36]. Then, R6G aqueous solution was added into each CdTe QDs solution with slightly stirring to obtain a series of R6G-QDs conjugates. The ratio (n) of concentration of QDs (C_{QDs}) to that of R6G (C_{R6G}) ($n = C_{QDs}/C_{R6G}$) in these conjugates was adjusted to 1:1, 2:1, 3:1, 4:1, 5:1, 7:1 and 10:1, respectively. R6G-QDs conjugates ($n = 10$) were selected for researching the relationship between ratiometric PL intensity of conjugates and concentration of added GSH (0.05–80 μM). All PL measurements of sample solutions were performed after incubating samples for 10 min in a black place at room temperature.

3. Results and discussion

3.1. PL properties of R6G-QDs conjugates

UV–vis absorption and PL emission spectra of R6G, CdTe QDs and R6G-QDs conjugates, were showed in Fig. 1. Markedly, absorption spectra of R6G-QDs conjugates displayed two shoulder peaks at 520 nM and 610 nM, which approached to characteristic peak sites of R6G and QDs. PL spectra of R6G partly overlaps with absorption spectra of QDs, which would induce fluorescence resonance energy transfer (FRET) from R6G to QDs in conjugates. As can be seen in Fig. 2a, PL intensity of R6G was reduced gradually by increased C_{QDs} in the range from 5 to 50 nM. It suggested the occurrence of a FRET donor-acceptor pair in R6G-QDs conjugates. Additionally, the increasing C_{QDs} resulted in the improvement of FRET efficiency (E). When the concentration ratio n (C_{QDs}/C_{R6G}) reached 10,

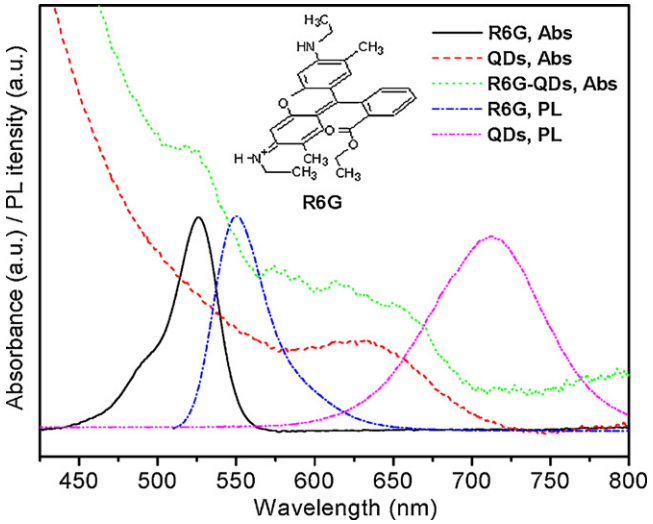

Fig. 1. UV–vis absorption spectra (Abs), fluorescence emission spectra (PL) of R6G, CdTe QDs and R6G-QDs conjugates, the excitation wavelength (λ_{ex}) is 500 nM.

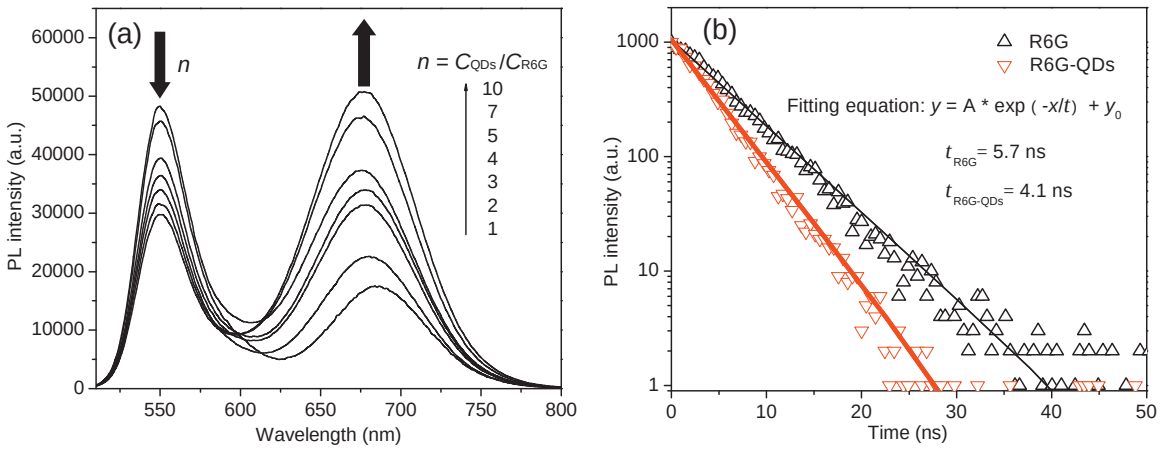

Fig. 2. (a) Evolutional PL spectra of conjugates of R6G (at 550 nM) and CdTe QDs (at 675 nM). (b) PL decay curves of sole R6G and R6G-QDs conjugates. PL lifetimes were obtained by single exponential curve fitting for R6G (black lines) and R6G-QDs (red lines). Emission wavelength (λ_{em}) was monitored at the first exitonic peak wavelength of R6G (at 550 nM). (For interpretation of the references to color in this figure legend, the reader is referred to the web version of the article.)

R6G-QDs conjugates showed a higher E (0.42) (Supporting information Fig. S1), and were utilized for a preferred FRET system in following experiments.

It is well known that the nonradiative exciton transfer is expected to substantially alter exciton lifetime properties of the donor and the acceptor. In particular, a comparison between measurements of exciton lifetimes of the donor alone and donor–acceptor pairs brought in close proximity, should provide information on FRET phenomenon [37]. Thus, to testify the FRET from R6G (as a donor) to QDs (as an acceptor), time resolved fluorescence decay curves of R6G were measured for sole R6G and R6G-QDs conjugates. As displayed in Fig. 2b, PL intensity of sole R6G and R6G-QDs conjugates exponentially decayed, and corresponding average PL lifetimes of R6G emission were 5.7 ns and 4.1 ns, respectively. The shorted PL lifetime of R6G should be attributed to the addition of QDs and the FRET process from R6G to QDs.

3.2. GSH induced PL response of R6G-QDs conjugates

There was a maximal E in R6G-QDs conjugates when the n reached 10. Thus, these conjugates could be used as a perfect FRET system for various applications. As demonstrated in Fig. 3,

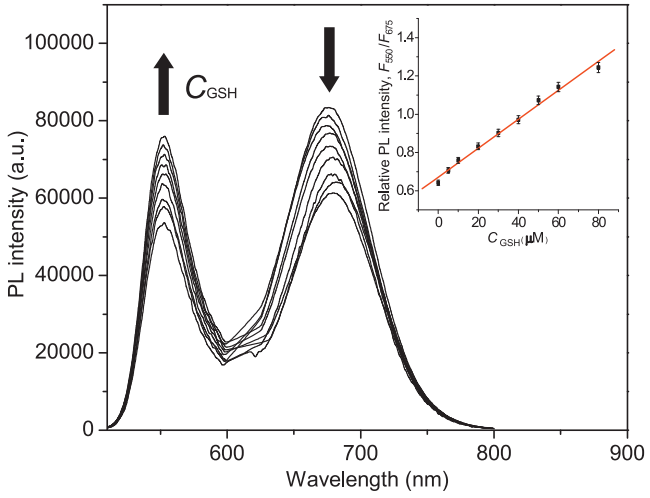

Fig. 3. Different PL spectra of R6G-QDs conjugates with each increment of C_{GSH} from 0.05 to 80 μM. Therein, C_{R6G} and C_{QDs} were 5 nM and 50 nM, respectively (λ_{ex} = 500 nM). Linear plot of the ratio of PL intensity at 550 nM (R6G, F_{550}) to that at 675 nM (QDs, F_{675}) versus the C_{GSH} were inserted.

the increasing C_{GSH} caused regular PL response of conjugates. In detail, the enhanced PL of R6G (at 550 nM) and reduced PL of QDs (at 675 nM) were observed. Furthermore, upon addition of GSH, the ratio of PL intensity of R6G to that of QDs (F_{550}/F_{675}) was near proportional toward the C_{GSH} in the range from 0.05 to 80 μM. The regression equation was $F_{550}/F_{675} = 0.007561 + 0.6715\ C_{GSH}$ (μM) with a good linear correlation coefficient (R) of 0.9954 and with a low average relative standard deviation of 2.1% (six repeats, C_{GSH} = 10 μM), as inserted in Fig. 3. The LOD of this proposed method was 15 nM, calculated by the 3σ, where σ is the standard deviation for six replicating detections of blank solutions. The LOD of 15 nM suggested that there was a no less than 40-fold enhancement in comparison with that of other QDs-based PL sensors in previous reports [28]. In view of this advantage, R6G-QDs conjugates-based ratiometric PL sensor was designed for highly sensitive detection of GSH.

In addition, temporal evolution of PL peak intensities of R6G-QDs conjugates with the addition of GSH (80 μM) at room temperature was investigated (Supporting information Fig. S2). Similar studies on the same conjugates, containing 0.05–60 μM of GSH, were performed to evaluate the relationship of final PL intensities and incubation time. As a result, ultima PL intensities of R6G and QDs were achieved after the addition of GSH for 10 min in a black place. It verified that GSH-induced PL evolution was rapid and could be developed as a PL sensor for rapid detection of GSH.

3.3. Mechanism of this ratiometric PL sensor

This conjugation of R6G and QDs could be attributed to electrostatic interactions between negatively charged —COO^- of MPA on the surface of QDs and cationic R6G in aqueous solution. Similar principle has been confirmed in recent reports of PL sensors. For instance, the negatively charged Calcein Blue anchored cationic polyelectrolyte polyethylenimine coated-luminescence CdTe nanorods [31,38]. Mercaptoacetic acid capped-CdSe/ZnS (core/shell) QDs fabricated the ion-pair with methyl viologen (MV^{2+}) [28].

Fig. 4 illuminated a clear work procedure of this R6G-QDs conjugates-based ratiometric PL sensor. Firstly, R6G and CdTe QDs were conjugated by electrostatic interactions in aqueous solution. The conjugation induced a FRET from R6G to QDs due to the overlapping between absorption spectrum of QDs and PL emission spectrum of R6G. Secondly, the addition of GSH destroyed this conjugation apparently by competitive chelation between GSH and MPA ligand on the surface of QDs. Hence, the PL of R6G

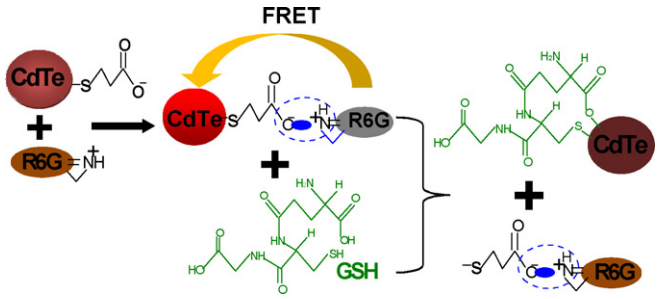

Fig. 4. Schematic representation of the work procedure of this R6G-QDs conjugates-based ratiometric PL sensor. Blue broken circle and blue dot represented conjugation area and electrostatic interaction, respectively. (For interpretation of the references to color in this figure legend, the reader is referred to the web version of the article.)

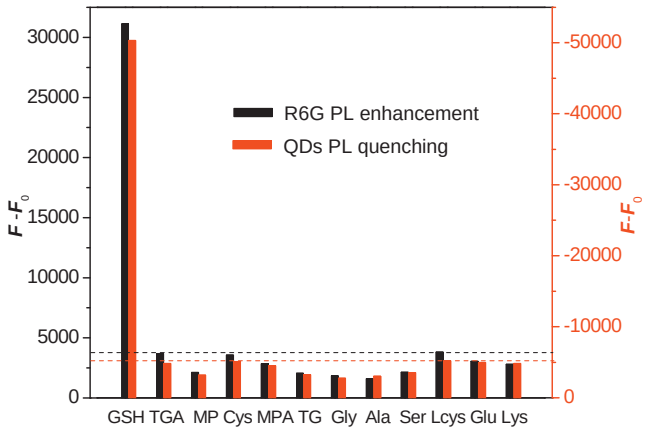

Fig. 6. PL response ($F - F_0$) at 550 nM (in black pillars) and at 675 nM (in red pillars) of R6G-QDs conjugates ($n = 10$) to diverse thiols and amino acids (80 μM) in 0.1 M of PBS (pH 7.4). Herein, F and F_0 represented PL intensity of conjugates before and after adding interferential molecules, respectively. (For interpretation of the references to color in this figure legend, the reader is referred to the web version of the article.)

was restored gradually. In literatures, the coordination chemistry of GSH involved two or more binding sites of the molecule (e.g. —SH and —COO^-). As a matter of fact, eight potential sites of GSH possessed chelation to metal ions (e.g. Cd^{2+}), and could lead to a stronger GSH-Cd^{2+} interaction than for other thiols and amino acids, containing single —SH or weak —COO^- or —NH_2 [39]. Further more, the larger steric hindrance effect of GSH helped to improve the stability to coordinate to metal ions [40].

UV–vis spectra of MPA-CdTe QDs in the presence of GSH and R6G were measured in Fig. 5a. The introduction of GSH and R6G brought out a slight red-shift of the absorption excitonic onset by 3 and 8 nM, respectively. For R6G-QDs conjugates, the addition of GSH gave rise to a 5 nM blue-shift of the absorption band, which was in great agreement with that of MPA-QDs with GSH. Corresponding average hydrodynamics diameters of four samples, as referred in Fig. 5a, were 7.1, 9.8, 13.5 and 10.1 nM, respectively (Supporting information Fig. S3). The near accordant spectral shift and size for "MPA-QDs + GSH" and "MPA-QDs + R6G + GSH" in our case suggested that resulting thiol-ligand exchange between MPA and GSH around QDs occurred, in company with partial loss of MPA-R6G conjugates.

To confirm the surface binding of capping molecules, powders of GSH and R6G-QDs conjugates were applied to record FTIR spectra in Fig. 5b. Bands at 1050 cm^{-1} and 3260 cm^{-1} were due to C—N stretching and N—H asymmetric stretching mode (in GSH) in spectra (I) and (III), respectively. A broad absorption peak at 3480 cm^{-1}, distinct bands at 2910 cm^{-1} and 1550 cm^{-1} were assigned to O—H vibration, C—H stretching vibrations of alkyl chains and vibration of carboxylate anion (in MPA molecules), respectively, as exhibited in spectra (II). The absence of S—H stretching mode at 2560 cm^{-1} in spectra (III) indicated that the —SH of GSH were bound to surface atoms of QDs by the Cd—S bond. Thus, it was inferred that the ligand exchange between MPA and GSH occurred in the course of adding GSH into R6G-QDs conjugates, and was responsible for regular PL change of conjugates upon the addition of GSH.

3.4. *Effect of interferential molecules on PL of R6G-QDs conjugates*

To demonstrate the selectivity of this R6G-QDs conjugates-based PL sensor, a series of competition experiments were implemented to determine PL intensity change of conjugates in the presence of other interferential thiols and amino acids, including MPA, thioglycolic acid (TGA), 2-mercaptoethand (MP), cysteamine (Cys), 1-thioglycerol (TG), glycine (Gly), alanine (Ala), serine (Ser), L-cysteine (Lcys), glutamic acid (Glu) and lysine (Lys). As shown in Fig. 6, PL responses of all competitors to these conjugates were rather slight (excluding GSH). In black pillars, enhanced PL (at 550 nM) from other competitors was less than 1/8 of that from GSH. In addition, in red pillars, reduced PL of conjugates (at 712 nM) due to addition of other competitors was no more than 1/10 of that from

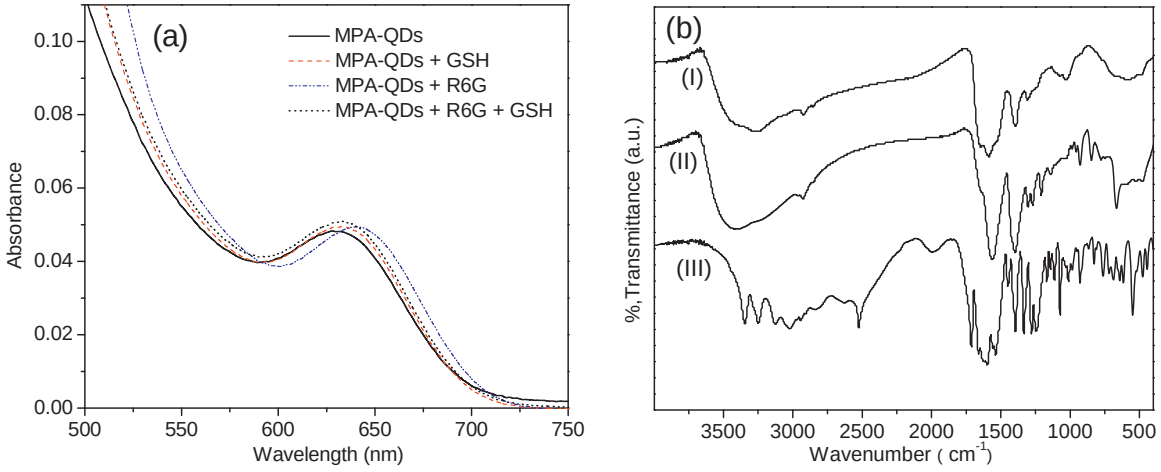

Fig. 5. (a) UV–vis spectra of MPA-capped CdTe QDs with addition of GSH and R6G. Herein, the concentration of QDs, R6G and GSH were 50 nM, 5 nM and 80 μM, respectively. (b) FTIR spectra of sole GSH (I) and R6G-QDs conjugates, containing 0 μM (II) and 80 μM (III) of GSH. All samples were loaded into KBr pellets.

Table 1
Test of the interference of various pH, ions, thiols and amino acids molecules on ratiometric PL intensity of R6G-QDs conjugates.

pH	CRI[a]	Ions	CC[b]	CRI	Molecules	CC	CRI
5.0	+2.9	Cl^-	5.0	−1.7	TGA	0.1	−3.5
5.5	+1.4	Br^-	5.0	−1.5	MP	1.0	−2.2
6.0	+0.8	I^-	5.0	−2.0	Cys	0.1	−3.1
6.5	+0.2	NO_3^-	5.0	+2.6	MPA	0.1	−0.9
7.0	−3.3	CO_3^{2-}	5.0	+1.6	TG	1.0	−0.5
7.4[c]	0	SO_4^{2-}	5.0	+1.2	Gly	1.0	−0.6
8.0	−4.7	Fe^{3+}	2.0	−2.7	Ala	1.0	+1.2
8.5	−3.2	Cu^{2+}	2.0	+3.8	Ser	1.0	−1.8
9.0	−1.9	Cd^{2+}	2.0	−4.2	Lcys	0.1	−3.7
		Pb^{2+}	2.0	+3.4	Glu	0.1	+0.1
		Hg^{2+}	2.0	+2.8	Lys	0.1	+0.3

[a] CRI: change of ratiometric PL intensity of R6G-QDs conjugates (%).
[b] CC: coexisting concentration (μM).
[c] pH 7.4: all interferential results were compared with the ratiometric PL of R6G-QDs conjugates upon the addition of 50 nM GSH in 10 mM of PBS at pH 7.4.

the addition of GSH. Although related biothiols, such as Lcys and Cys, exhibited similar PL tendency, the sensitivity was much lower than for GSH in the same quantitative detection area. The differentia of sensitivities was ascribed to the distinct coordination capability and steric hindrance effects. Due to possessing the stronger coordination and larger steric hindrance effect, GSH induced the more swift PL response of R6G-QDs conjugates than that of other thiols [39–41]. Indubitability, these results richly confirmed that PL intensity response of R6G-QDs conjugates was of high selectivity toward C_{GSH}, and the presence of other thiols or amino acids only resulted in slight perturbation or fluctuation on measuring PL intensity of these conjugates.

3.5. Effect of pH, ions and molecules on ratiometric PL of conjugates

To further confirm the selectivity of this R6G-QDs conjugates-based ratiometric PL sensor, a variety of pH, ions and interferential molecules were researched to evaluate their influence on this sensor. The experiment was carried out by fixing C_{GSH} to 50 nM in 10 mM of PBS, and then recording ratiometric PL intensity of conjugates before (F_0) and after (F) adding foreign interferential ingredients. The tolerance level was defined as the resulting change of ratiometric PL intensity (CRI, %) = $(F - F_0)/F_0 \times 100$ less than ±5%. Determinated results from these interferential experiments were summarized in Table 1. According to these results, the pH hardly interfered the CRI of R6G-QDs conjugates in the range from pH 5.0 to 9.0. The interference of inorganic ions was investigated and was found to be rather slight (CRI < ±5%) at the coexisting concentration (CC) up to 2 μM or 5 μM. In general, 2 μM is a normal concentration level in most detection situations, especially in biological organisms [28]. In addition, the CRI of this conjugate from addition of other thiols and amino acids was also less than ±5% at the CC up to 0.1 μM or 1 μM. These results adequately testified that this R6G-QDs conjugates-based ratiometric PL sensor for the determination of GSH was highly selective in the presence of other interferential ingredients at the CC up to a much higher value than the C_{GSH}.

3.6. Analytical performance of this PL sensor in mixture solutions and biological samples

Application experiments are crucial for evaluating analytical performance of this PL sensor because of possible influence from naturally existing molecules and interferences. A series of real samples were regularly analyzed to examine the feasibility of the proposed method, including mixture solutions and biological samples with both the analyte and interfering species. As summarized in Table 2, all measured results from the PL sensor were in good agreement with those obtained by HPLC. Detected concentrations of GSH from the sensor and HPLC were close to intentionally added C_{GSH}. Further more, the relative standard deviation (RSD) from mixture solution determinations by the sensor was in the range from 1.9% to 4.2% (by HPLC, 0.8–7.7%). In addition, a series of liposome and BSA aqueous solutions were prepared, as naturally biological samples, as displayed in Table 3. All detected results from the sensor and HPLC were in good agreement with added GSH. The RSD from the sensor was in the range from 1.8% to 4.2% (for HPLC, 0.9–8.5%).

Table 2
Analytical results of GSH in mixture solutions achieved by PL sensor and HPLC.

Samples[a]	pH	Added GSH (μM)	By PL sensor[b] (μM)	RSD[c] (%)	By HPLC (μM)	RSD (%)
Mixture 1	6.0	5.0	4.8 ± 0.2	4.2	5.2 ± 0.4	7.7
	7.4	5.0	5.3 ± 0.1	1.9	5.4 ± 0.2	3.7
	8.0	5.0	5.1 ± 0.2	3.9	4.7 ± 0.3	6.4
Mixture 2	6.0	80.0	77.6 ± 2.3	3.0	78.5 ± 1.1	1.4
	7.4	80.0	82.7 ± 1.9	2.3	77.9 ± 1.3	1.7
	8.0	80.0	79.7 ± 1.5	1.9	82.8 ± 0.7	0.8

[a] Mixture samples were prepared by mixing interferential components together in 10 mM of PBS at pH 6.0, 7.4 and 8.0, respectively, containing Cl^- (5 μM), CO_3^{2-} (5 μM), Cu^{2+} (2 μM), Pb^{2+} (2 μM), TGA (0.1 μM), Cys (0.1 μM), Lcys (0.1 μM), Glu (0.1 μM) and GSH (5 μM or 80 μM).
[b] Measured GSH were expressed as mean of six determinations ±standard deviation (SD).
[c] The relative standard deviation (RSD) was calculated as (SD/mean) × 100%.

Table 3
Analytical performance of GSH in a series of liposome and BSA aqueous samples.

Samples[a] (mM)	Added (μM)	By sensor (μM)	RSD (%)	By HPLC (μM)	RSD (%)
Liposome 1 (1.0)	5.0	4.9 ± 0.2	4.1	5.1 ± 0.2	3.9
Liposome 2 (1.0)	80.0	77.8 ± 1.8	2.3	81.6 ± 1.2	1.5
Liposome 3 (2.0)	5.0	5.3 ± 0.1	1.9	4.7 ± 0.4	8.5
Liposome 4 (2.0)	80.0	78.6 ± 2.1	2.7	79.1 ± 1.5	1.9
BSA 1 (1.0)	5.0	5.4 ± 0.2	3.7	4.8 ± 0.1	2.1
BSA 2 (1.0)	80.0	82.5 ± 1.5	1.8	81.0 ± 0.8	0.9
BSA 3 (2.0)	5.0	4.9 ± 0.1	2.0	5.0 ± 0.2	4.0
BSA 4 (2.0)	80.0	78.5 ± 1.7	2.2	79.6 ± 1.1	1.4

[a] All biological samples were prepared by dissolving liposome and BSA in 10 mM of PBS at pH 7.4.

Remarkably, the facile sensor could substitute complicated HPLC for detection of GSH in our case.

Consequently, it is concluded that the coexistence of other interferential ions and molecules in mixture solutions hardly affects the detection of GSH. Especially, the sensor exhibited a great tolerance in biological samples, which further proved the practicability of this sensor.

4. Conclusions

In summary, facile, economic, highly selective and sensitive R6G-QDs conjugates-based ratiometric PL sensor were developed to determine GSH. The PL, UV–vis, FTIR spectra, PL lifetimes and DLS techniques testified the occurrence of FRET behavior (from R6G to QDs) and the thiol-ligand exchange process (from MPA to GSH). Interferential experiments revealed that the ratiometric PL (F_{550}/F_{675}) of the sensor presented high selectivity over other related thiols and amino acids, pH and common ions. Corresponding calibration plot of F_{550}/F_{675} versus C_{GSH} was near proportional with a good linear coefficient of 0.9955 in the C_{GSH} range from 0.05 to 80 μM. The LOD of this proposed method was about 15 nM, which was almost 40-fold lower than that of other QDs-based PL sensors for the determination of GSH. Real assays in mixture solutions and biological samples suggested that this facile sensor was of perfect performance and could replace complex HPLC in our case. This proposed method could be used to develop other types of QDs-based molecular or ionic probes for ratiometric PL sensing, and was beneficial to the in-depth research of GSH levels in biological samples and biomedical systems.

Acknowledgments

This work was financially supported by the National Natural Science Foundation of China (nos. 20673059 and 20573056), the National High-Tech Research and Development Plan of China ("863" plan no. 2011AA06A107), the Nature Science Keystone Foundation of Shanghai (08jc1408100), the Fundamental Research Funds for the Central Universities of China (WK0913002) and the Nanotechnology Special Program Foundation of Shanghai (0652nm010).

Appendix A. Supplementary data

Supplementary data associated with this article can be found, in the online version, at http://dx.doi.org/10.1016/j.talanta.2012.03.043.

References

[1] A. Meister, M.E. Anderson, Annu. Rev. Biochem. 52 (1983) 711–760.
[2] A. Meister, Science 220 (1983) 472–477.
[3] M.E. Johll, D.G. Willimas, S.C. Johnson, Electroanalysis 9 (1997) 1397–1402.
[4] X.P. Chen, R.F. Cross, A.G. Clark, W.L. Baker, Mikrochim. Acta 130 (1999) 225–231.
[5] T. Mourad, K.L. Min, J.P. Steghens, Anal. Biochem. 283 (2000) 146–152.
[6] A.R. Ivanov, I.V. Nazimov, L.A. Baratova, J. Chromatogr. A 870 (2000) 433–442.
[7] M. Pohanka, H. Bandouchova, J. Sobotka, J. Sedlackova, I. Soukupova, J. Pikula, Sensors 9 (2009) 9094–9103.
[8] M. Pohanka, H. Band'ouchova, K. Vlckova, J.Z. Karasova, K. Kuca, V. Damkova, L. Peckova, F. Vitula, J. Pikula, J. Appl. Biomed. 9 (2011) 103–109.
[9] S.J. Chen, H.T. Chang, Anal. Chem. 76 (2004) 3727–3734.
[10] W.L. Wong, K.H. Huang, P.F. Teng, C.S. Lee, H.L. Kwong, Chem. Commun. (2004) 384–385.
[11] K. Gong, X. Zhu, R. Zhao, S. Xiong, L. Mao, C. Chen, Anal. Chem. 77 (2005) 8158–8165.
[12] P.K. Sudeep, S.T.S. Joseph, K.G. Thomas, J. Am. Chem. Soc. 127 (2005) 6516–6517.
[13] B. Tang, Y. Xing, P. Li, N. Zhang, F. Yu, G. Yang, J. Am. Chem. Soc. 129 (2007) 11666–11667.
[14] M. Zhang, M. Yu, F. Li, M. Zhu, M. Li, Y. Gao, L. Li, Z. Liu, J. Zhang, D. Zhang, T. Yi, C. Huang, J. Am. Chem. Soc. 129 (2007) 10322–10323.
[15] E.M. All, Y. Zheng, H.H. Yu, J.Y. Ying, Anal. Chem. 79 (2007) 9452–9458.
[16] J. Bouffard, Y. Kim, T.M. Swager, R. Weissleder, S.A. Hilderbrand, Org. Lett. 10 (2008) 37–40.
[17] J.S. Lee, P.A. Ulmann, M.S. Han, C.A. Mirkin, Nano Lett. 8 (2008) 529–533.
[18] K.S. Lee, T.K. Kim, H.G. Lee, H.J. Kim, J.I. Hong, Chem. Commun. (2008) 6173–6175.
[19] S. Huang, Q. Xiao, Z. He, Y. Liu, P. Tinnefeld, X. Su, X. Peng, Chem. Commun. (2008) 5990–5992.
[20] V.A. Hong, A. Kislukhin, M.G. Finn, J. Am. Chem. Soc. 131 (2009) 9986–9994.
[21] S. Banerjee, S. Kar, J.M. Perez, S. Santra, J. Phys. Chem. C 113 (2009) 9659–9663.
[22] H. Chen, J. Fu, L. Wang, B. Ling, B. Qian, J. Chen, C. Zhou, Talanta 83 (2010) 139–144.
[23] G. Liang, H. Liu, J. Zhang, J. Zhu, Talanta 80 (2010) 2172–2176.
[24] Q. Zhao, F. Li, C. Huang, Chem. Soc. Rev. 39 (2010) 3007–3030.
[25] Q. Ma, E. Ha, F. Yang, X. Su, Anal. Chim. Acta 701 (2011) 60–65.
[26] H. Zhang, B. Jiang, Y. Xiang, Y. Zhang, Y. Chai, R. Yuan, Anal. Chim. Acta 688 (2011) 99–103.
[27] Y. Wang, J. Lu, L. Tang, H. Chang, J. Li, Anal. Chem. 81 (2009) 9710–9715.
[28] J. Liu, C. Bao, X. Zhong, C. Zhao, L. Zhu, Chem. Commun. 46 (2010) 2971–2973.
[29] J. Lei, L. Wang, J. Zhang, Chem. Commun. 46 (2010) 8445–8447.
[30] T. Jin, A. Sasaki, M. Kinjo, J. Miyazaki, Chem. Commun. 46 (2010) 2408–2410.
[31] M. Liu, H. Zhao, X. Quan, S. Chen, H. Yu, Chem. Commun. 46 (2010) 1144–1146.
[32] G.J. Kim, K. Lee, H. Kwon, H.J. Kim, Org. Lett. 13 (2011) 2799–2801.
[33] J. Pan, D. Wan, J. Gong, Chem. Commun. 47 (2011) 3442–3444.
[34] Z. Gu, L. Zou, Z. Fang, W. Zhu, X. Zhong, Nanotechnology 19 (2008) 135604–135610.
[35] L. Zou, Z. Gu, N. Zhang, Y. Zhang, Z. Fang, W. Zhu, X. Zhong, J. Mater. Chem. 18 (2008) 2807–2815.
[36] W.W. Yu, L.H. Qu, W.Z. Guo, X.G. Peng, Chem. Mater. 15 (2003) 2854–2860.
[37] A.R. Clapp, I.L. Medintz, J.M. Mauro, B.R. Fisher, M.G. Bawendi, H. Mattoussi, J. Am. Chem. Soc. 126 (2004) 301–310.
[38] N.Q. Jia, Q. Lian, H.B. Shen, C. Wang, X.Y. Li, Z.N. Yang, Nano Lett. 7 (2007) 2976–2980.
[39] M.S. Diaz-Cruz, F. Mendieta, R. Tauler, M. Esteban, J. Inorg, Biochemistry 66 (1997) 29–36.
[40] B.Y. Han, J.P. Yuan, E.K. Wang, Anal. Chem. 81 (2009) 5569–5573.
[41] Y. Zhang, Y. Li, X.P. Yan, Anal. Chem. 81 (2009) 5001–5007.